# Supporting Information

### X-Ray structure determination

Diffraction data were collected exploring over a hemisphere of the reciprocal space in a combination of φ and ω scans to reach a resolution of 0.86 Å, using a Bruker APEX2[1] software suite (each exposure of 40 s covered 1° in ω. Unit cell dimensions were determined for least-squares fit of reflections with $I > 20\sigma$. A semi-empirical absorption and scale correction based on equivalent reflection was carried out using SADABS.[2] The space group determination was carried out using XPREP.[3] The structures were solved by direct methods. The final cycles of refinement were carried out by full-matrix least-squares analyses with anisotropic thermal parameters of all non-hydrogen atoms. The hydrogen atoms were fixed at their calculated positions using distances and angle constraints. All calculations were performed using SMART[4]and APEX2[1] software for data collection, SAINT[2] for data reduction, and SHELXTL[3] to resolve and refine the structure.

**Table S1** Main crystallographic and refinement data for compounds **InPF-12** to **InPF-15**.

| **Formula** | **InPF-12** $C_{75}H_{44}F_{18}N_4O_{14}In_2$ | **InPF-13** $C_{71}H_{44}F_{18}N_4O_{14}In_2$ | **InPF-14** $C_{61}H_{32}F_{18}N_2O_{12}In_2$ | **InPF-15** $C_{78}H_{44}F_{24}N_2O_{20.35}In_4$ |
|---|---|---|---|---|
| Molecular Weight /gmol$^{-1}$ | 1796.78 | 1748.74 | 1556.53 | 2252.43 |
| Temperature/K | 296(2) | 293(2) | 293(2) | 296(2) |
| Wavelength/Å | Cu Kα | Cu Kα | Cu Kα | Cu Kα |
| Crystal System | Monoclinic | Monoclinic | Monoclinic | Monoclinic |
| Space Group | *C2/c* | *C2/c* | *C2/c* | *P2$_1$/n* |
| a/Å | 33.0893(4) | 32.6149(5) | 38.278(1) | 24.165(2) |
| b/Å | 12.9108(2) | 12.4824(2) | 7.7778(2) | 13.456(1) |
| c/Å | 22.2089(3) | 21.4240(3) | 26.8178(8) | 27.388(3) |
| α/° | 90 | 90 | 90 | 90 |
| β/° | 129.956(1) | 129.055(1) | 129.831(1) | 111.227(6) |
| γ/° | 90 | 90 | 90 | 90 |
| V/Å$^3$ | 7272.8(2) | 6773.0(2) | 6131.4(3) | 8301.6(1) |
| Z | 4 | 4 | 4 | 4 |
| Dx/ g.cm$^{-3}$ | 1.641 | 1.715 | 1.686 | 1.802 |
| μ/mm$^{-1}$ | 6.088 | 6.516 | 7.076 | 9.905 |
| F(000) | 3576 | 3480 | 3072 | 4408 |
| GOF F$^2$ | 0.995 | 1.056 | 1.040 | 1.014 |
| Final R indices [I>2σ(I)] | R1=0.0336<br>wR2=0.0888 | R1=0.0382<br>wR2=0.0913 | R1=0.0484<br>wR2=0.1165 | R1=0.0532<br>wR2=0.1049 |
| R indices (all data) | R1=0.0422<br>wR2=0.0953 | R1=0.0494<br>wR2=0.0969 | R1=0.0707<br>wR2=0.1308 | R1=0.0927<br>wR2=0.1210 |

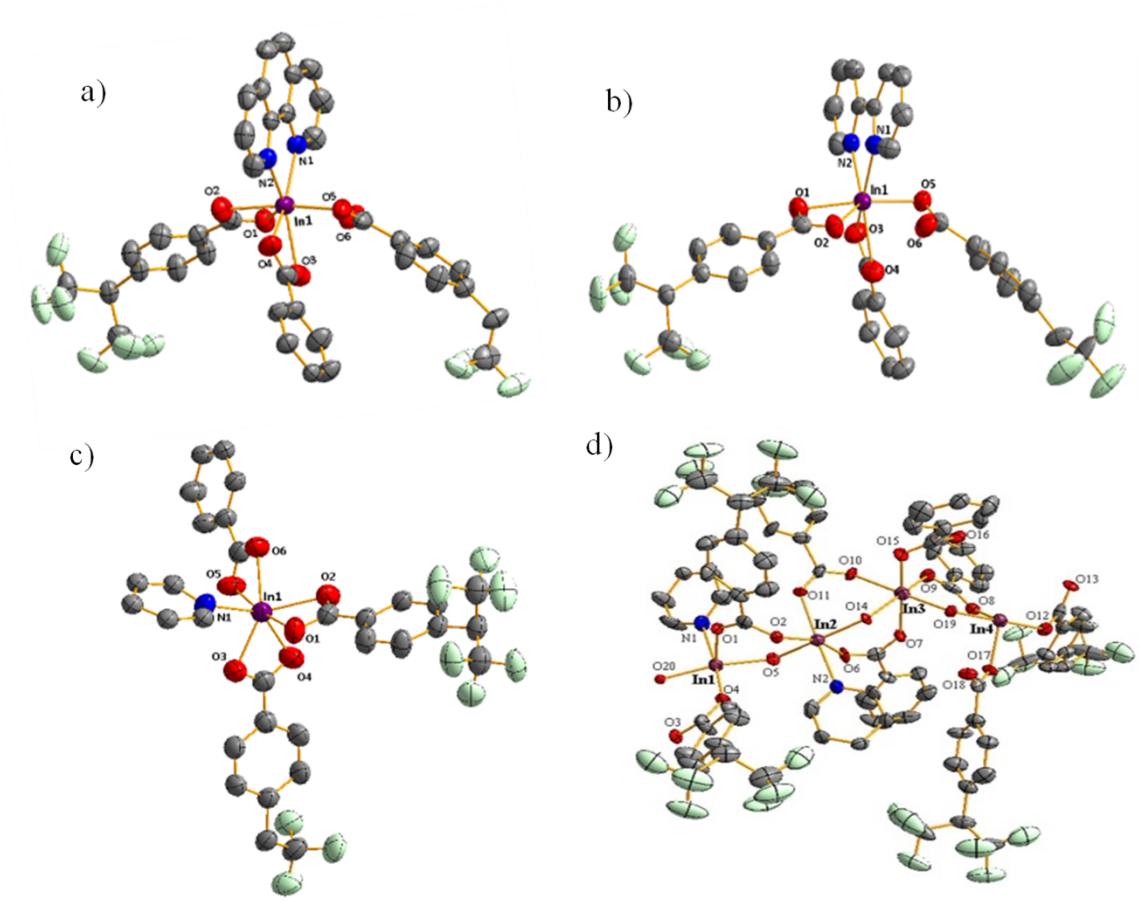


Fig. S1 ORTEP representation of asymmetric units for compounds InPF-12 (a), InPF-12 (b), InPF-14 (c) and InPF-15 (d). Ellipsoids are displayed at the 50% probability level Hydrogen atoms and water molecules were omitted for clarity.

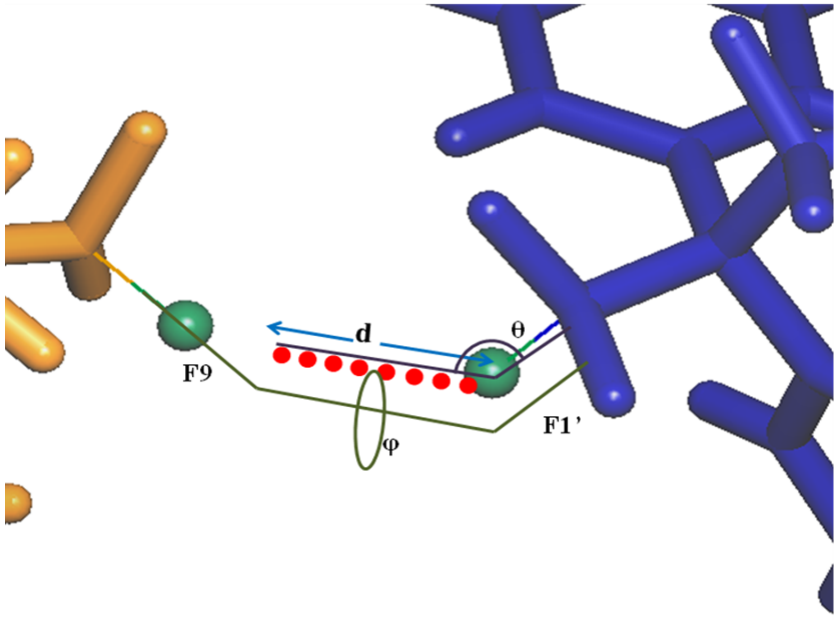


d F9···F1' = 2.723Å  d C26-F9···F1' = 3.805Å  d C9'-F1'···F9 = 3.552Å
$\theta_1$: 117.96°  $\theta_2$: 153.41°  φ: 26.32°

Fig S2 View of the weak F•••F interactions found in InPF-12.

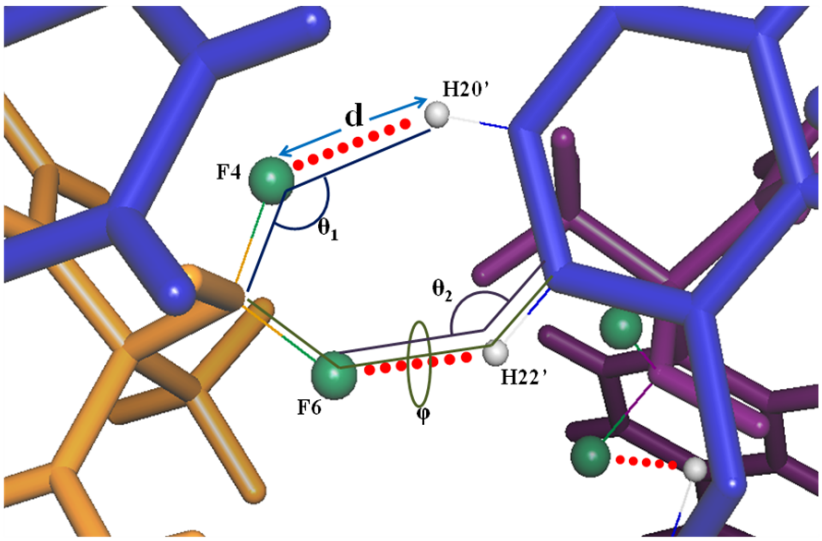


Fig. S3 View of the weak C-H•••F interactions found in InPF-13.

**CG-MS for Catalytic Product Characterization**

In order to identify the principal product in the cyanosilylation reaction and obtain the conversion yield, small amounts of catalytic sample at different reaction times were analyzed through CG-MS. The yields reported in the document tables were determined by the area under the curve in the reported chromatogram.

(a) 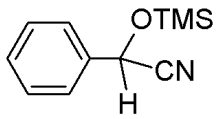

$C_{11}H_{15}NOSi$
205.33g/mol

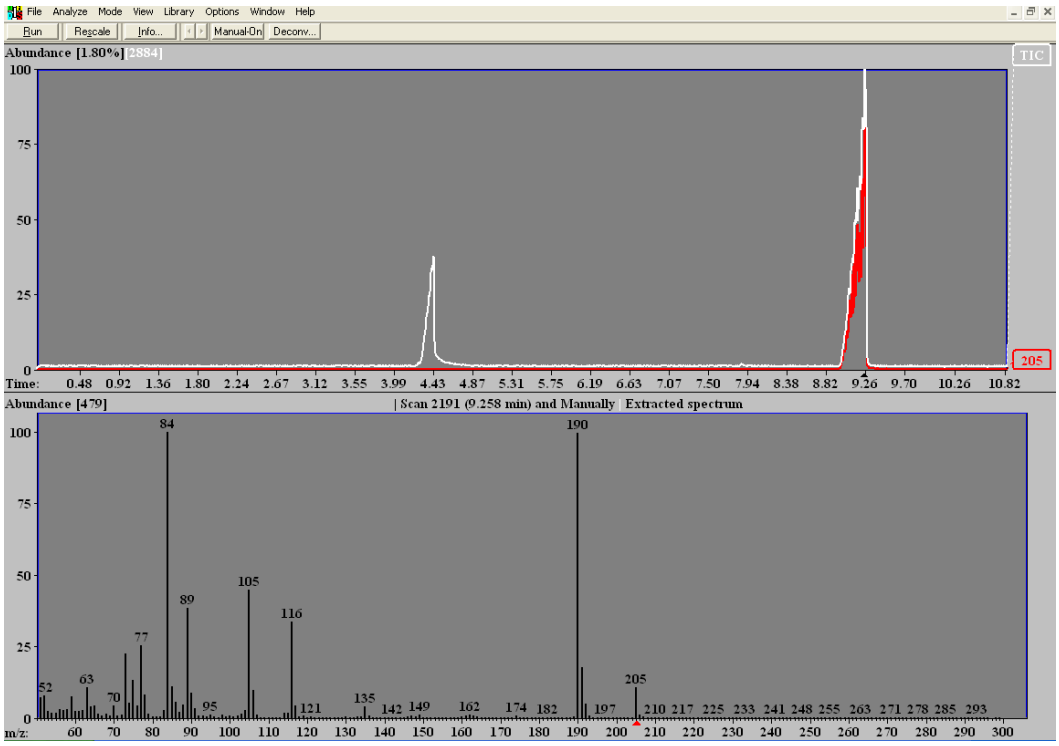


Fig. S4 View of the CG-MS for the cyanohydrin (a)

(b)

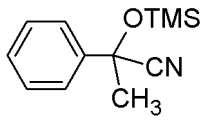


$C_{12}H_{17}NOSi$
219.35g/mol

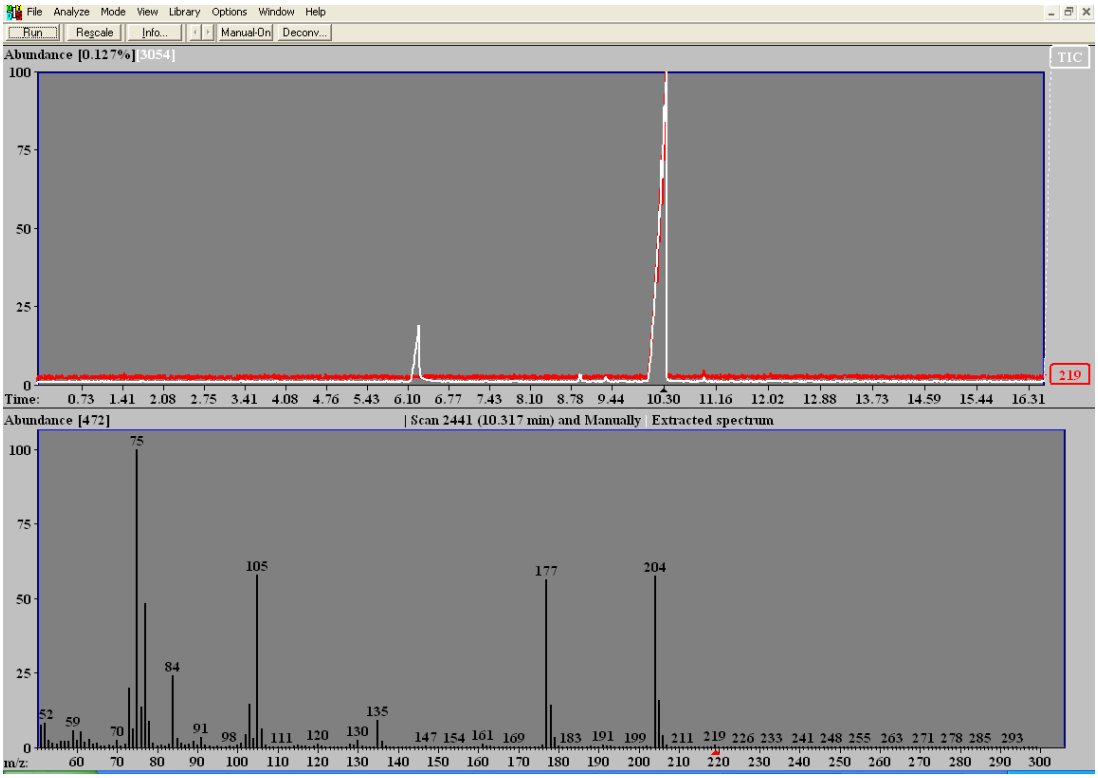


Fig. S5 View of the CG-MS for the cyanohydrin (b)

(c)

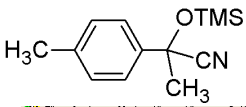


$C_{13}H_{19}NOSi$
233.38g/mol

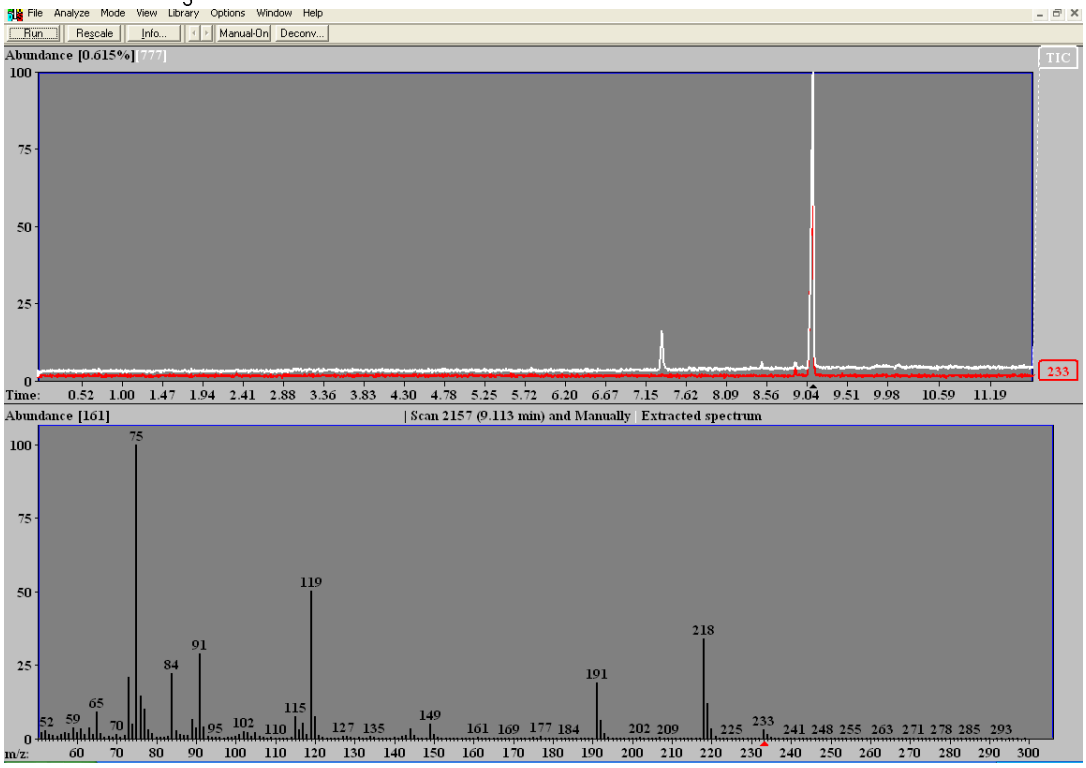


Fig. S6 View of the CG-MS for the cyanohydrin (c)

(d)

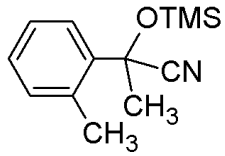


$C_{13}H_{19}NOSi$
233.38g/mol

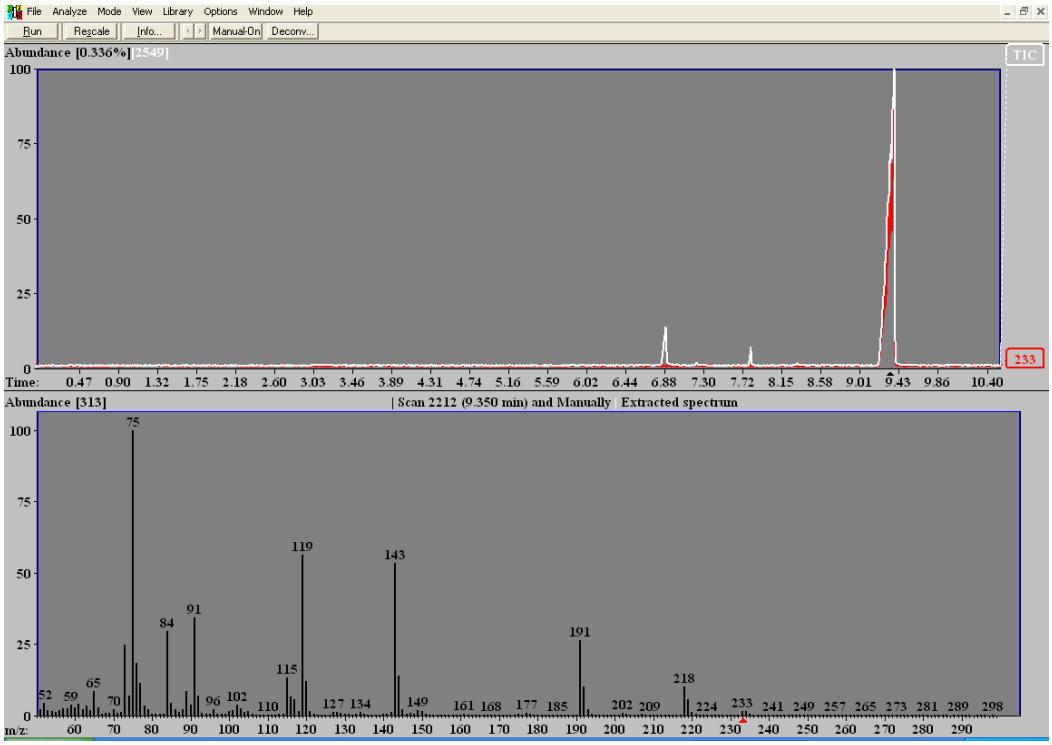


Fig. S7 View of the CG-MS for the cyanohydrin (d)

(e)

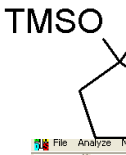


$C_9H_{17}NOSi$
183.32g/mol

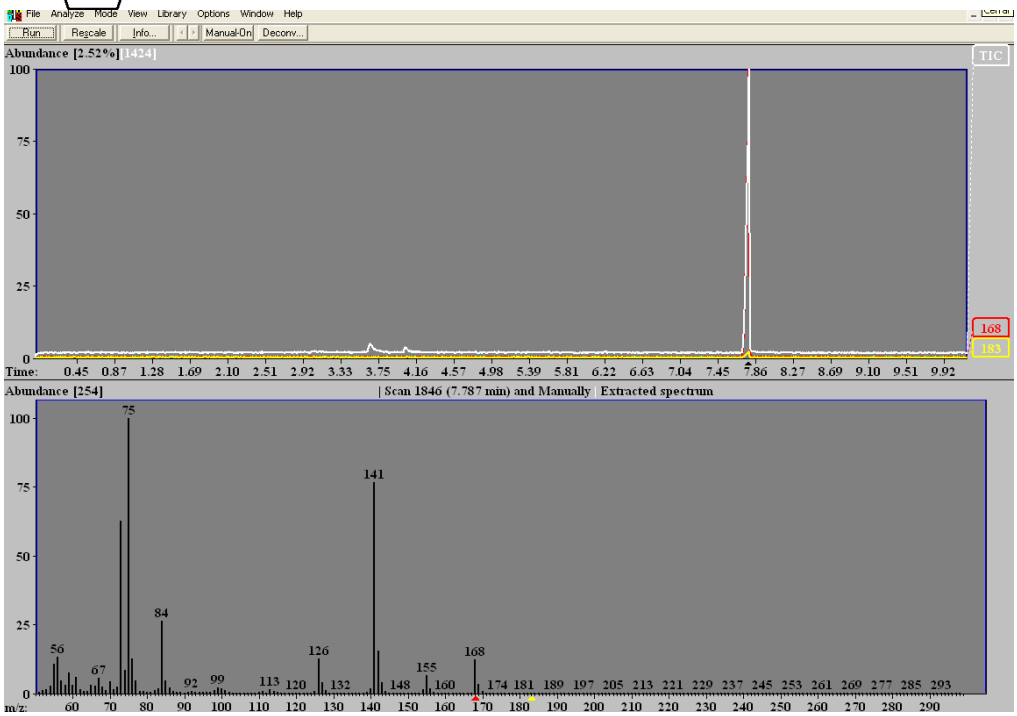


Fig. S8 View of the CG-MS for the cyanohydrin (e)

(f)


$C_{10}H_{19}NOSi$
197.35g/mol

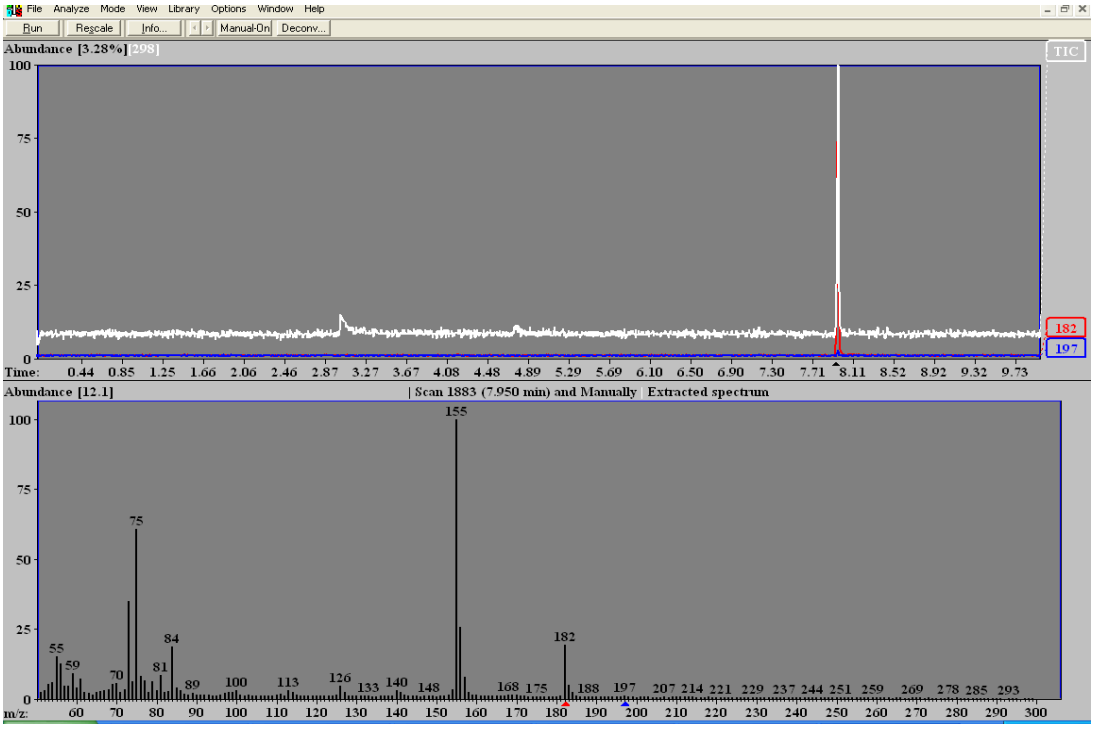


Fig. S9 View of the CG-MS for the cyanohydrin (f)

(g)

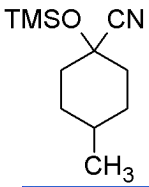


$C_{11}H_{21}NOSi$
211.38g/mol

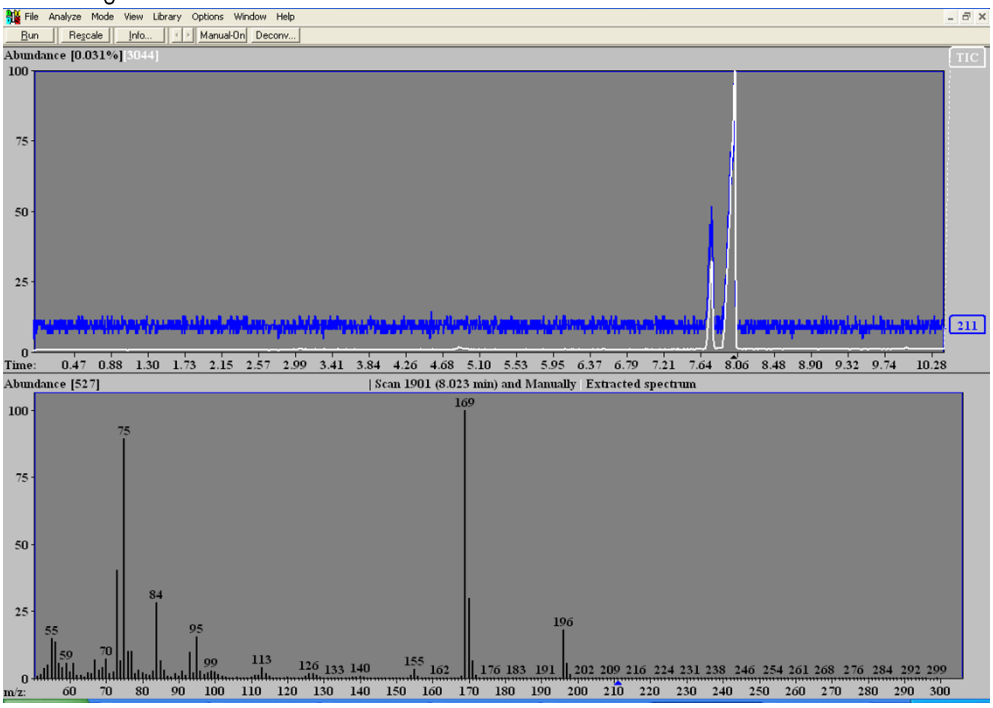


Fig. S10 View of the CG-MS for the cyanohydrin (g)

(h)

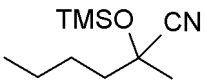


$C_{10}H_{21}NOSi$
199.36g/mol

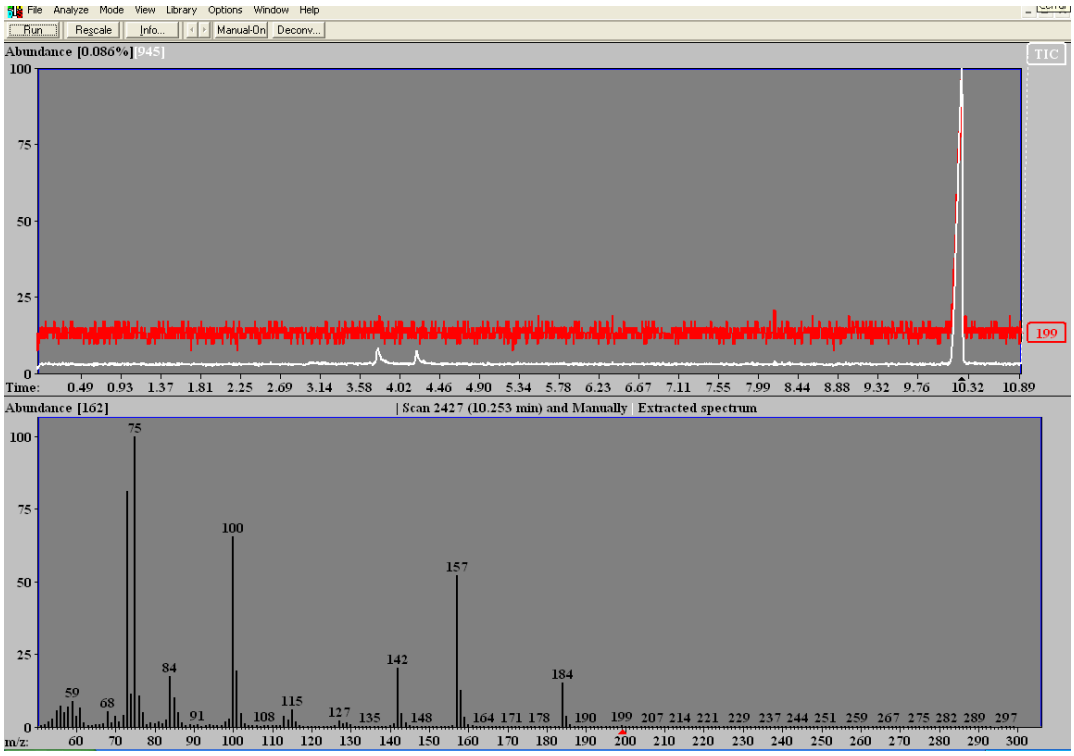


Fig. S11 View of the CG-MS for the cyanohydrin (h)

(i)

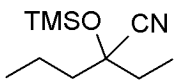


$C_{10}H_{21}NOSi$
199.36g/mol

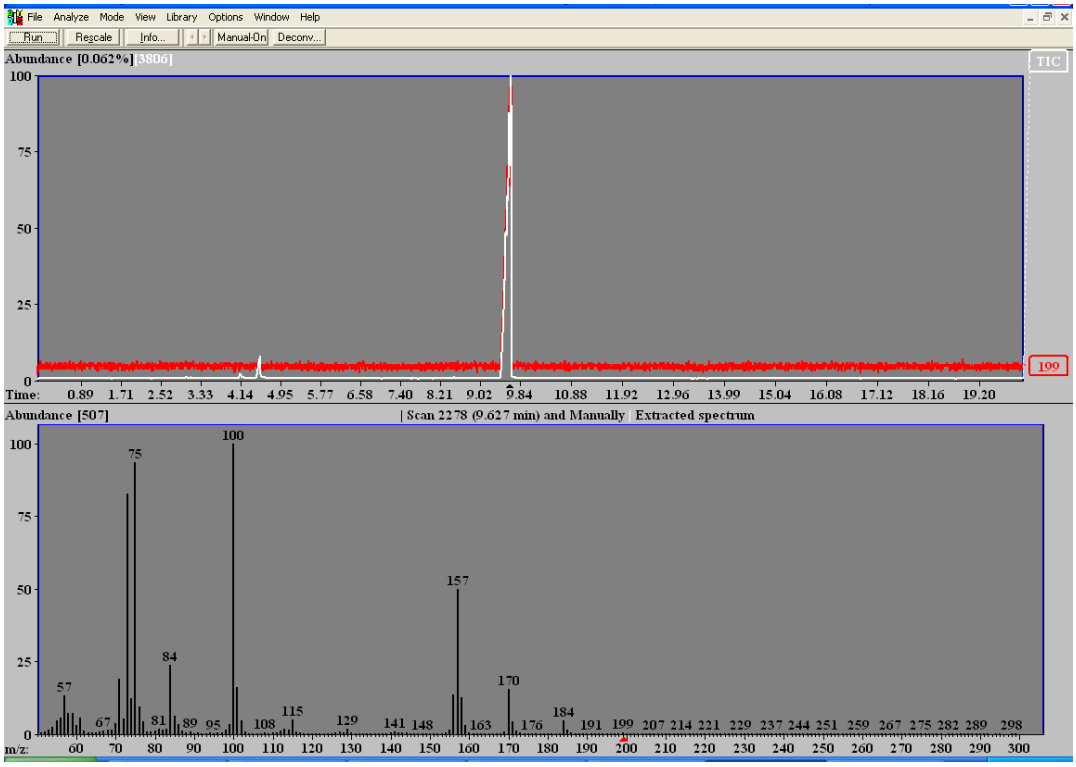


Fig. S12 View of the CG-MS for the cyanohydrin (i)

**Characterization methods**

IR: Infrared spectra were recorder from KBr pellets in the range 4000-250 $cm^{-1}$ on a Bruker IFS 66V/S. TGA-DTA: Thermogravimetric and differential thermal analyses were performed using a Seiko TG/DTA 320U equipment in a temperature range between 25 and 1000 ºC in air (100 mL/min flow) and heating rate of 10ºC/min. The residues of the compounds after TGA were analyzed by PXRD and compared with inorganic crystal structure database (ICSD)[5] patterns reported. EA: A Perkin-Elmer CNHS Analyzer 2400 was employed for the elemental analysis. PXRD: Powder X-ray diffraction patterns were measured with a Bruker D8 diffractometer, with step size = 0.02 º and exposure time = 0.5 s/step. PXRD measurements were used to check the purity of the obtained microcrystalline products by a comparison of the experimental results with the simulated patterns obtained from single-crystal X-ray diffraction data.

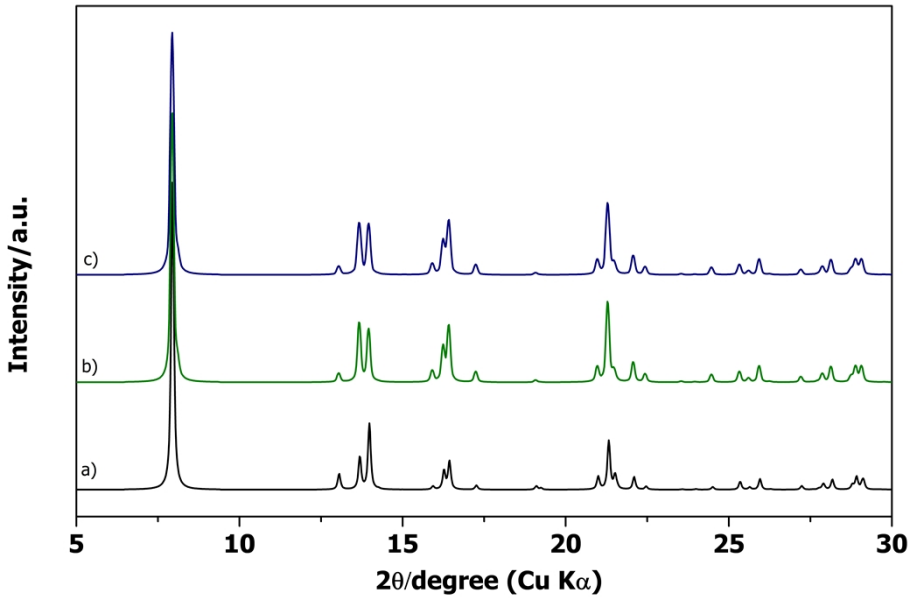


Fig. S13 Normalized PXRD patterns of InPF-11: a) simulated PXRD, b) experimental PXRD and c) PXRD after the first run of cyanosilylation catalysis.

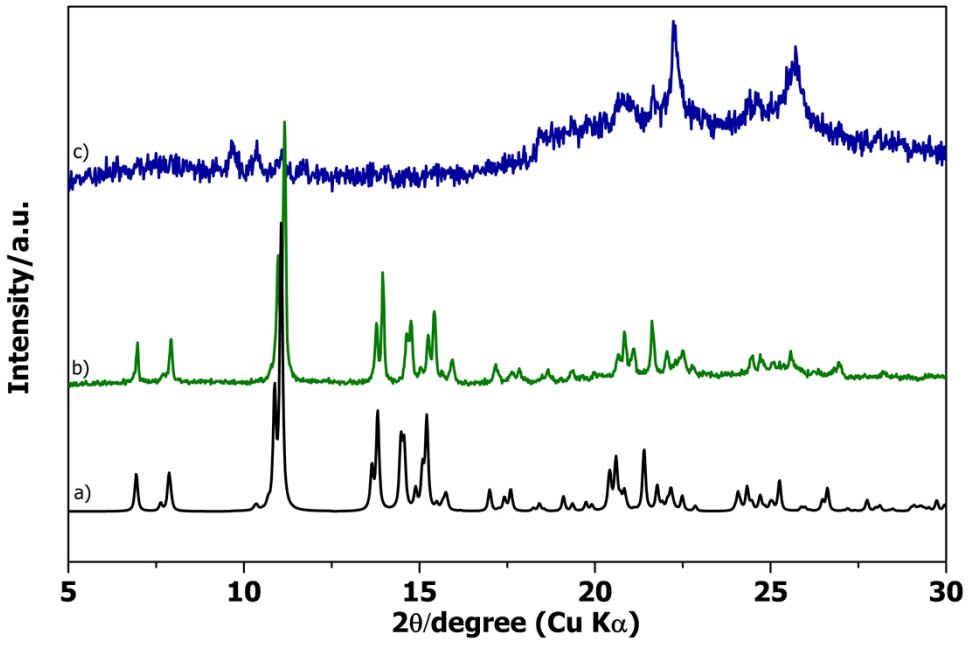


Fig. S14 Normalized XRD patterns of InPF-12: a) simulated PXRD, b) Experimental PXRD and c) PXRD after the first run of cyanosilylation catalysis.

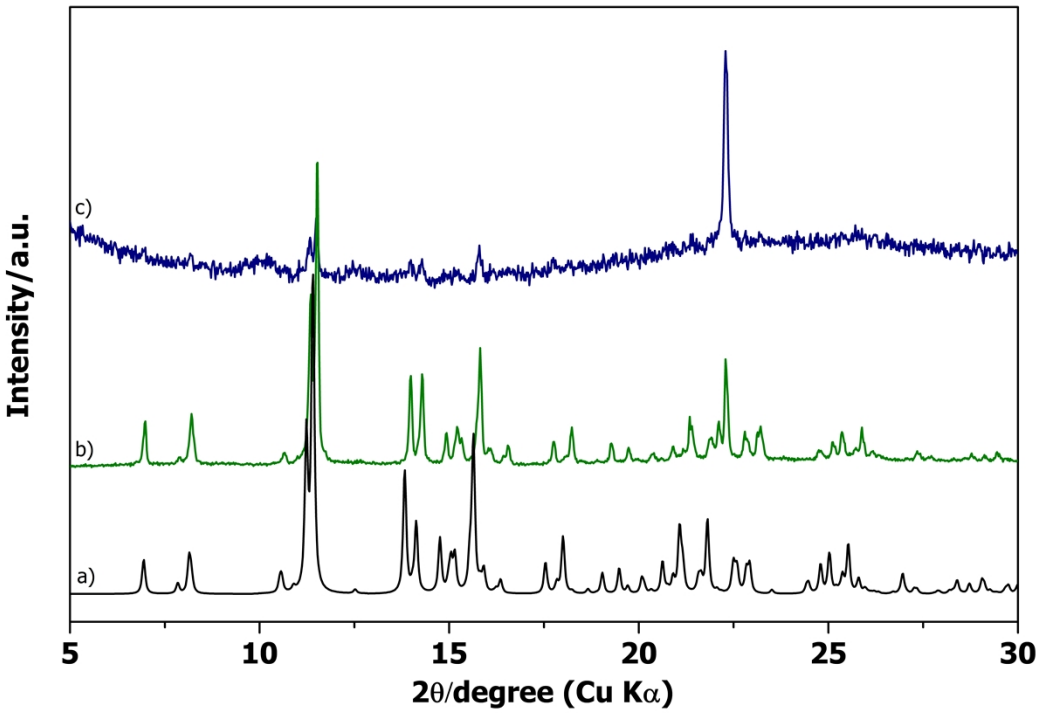


Fig. S15 Normalized XRD patterns of InPF-13: a) simulated PXRD, b) Experimental PXRD and c) PXRD the after first run of cyanosilylation catalysis.

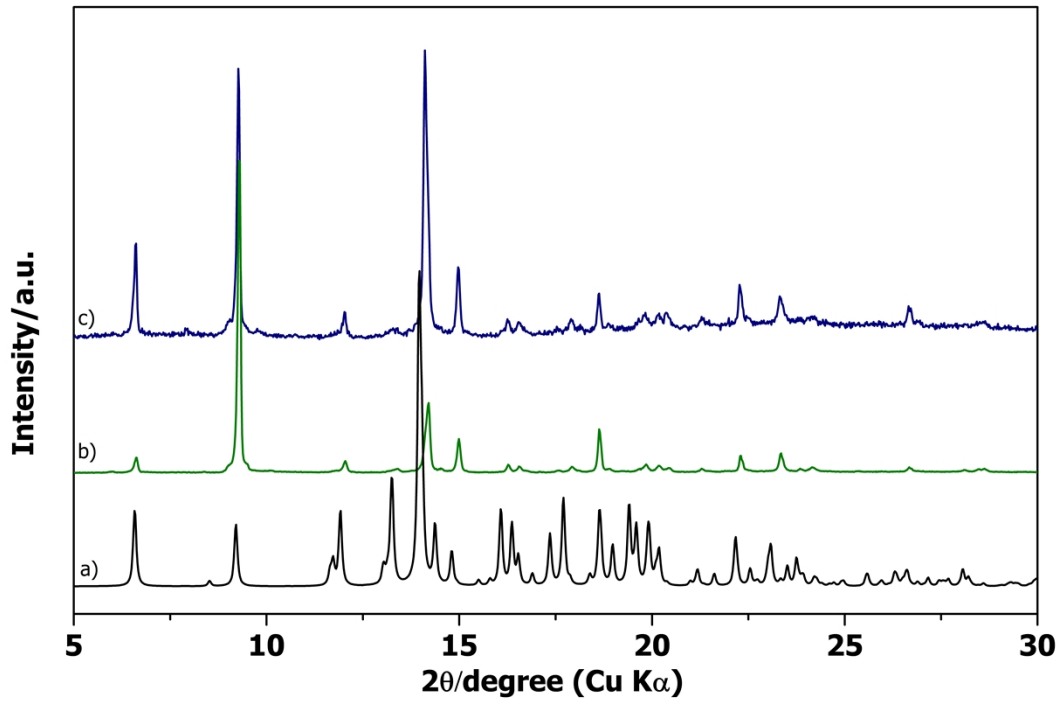


Fig. S16 Normalized XRD patterns of InPF-14: a) simulated PXRD, b) Experimental PXRD and c) PXRD after the first run of cyanosilylation catalysis.

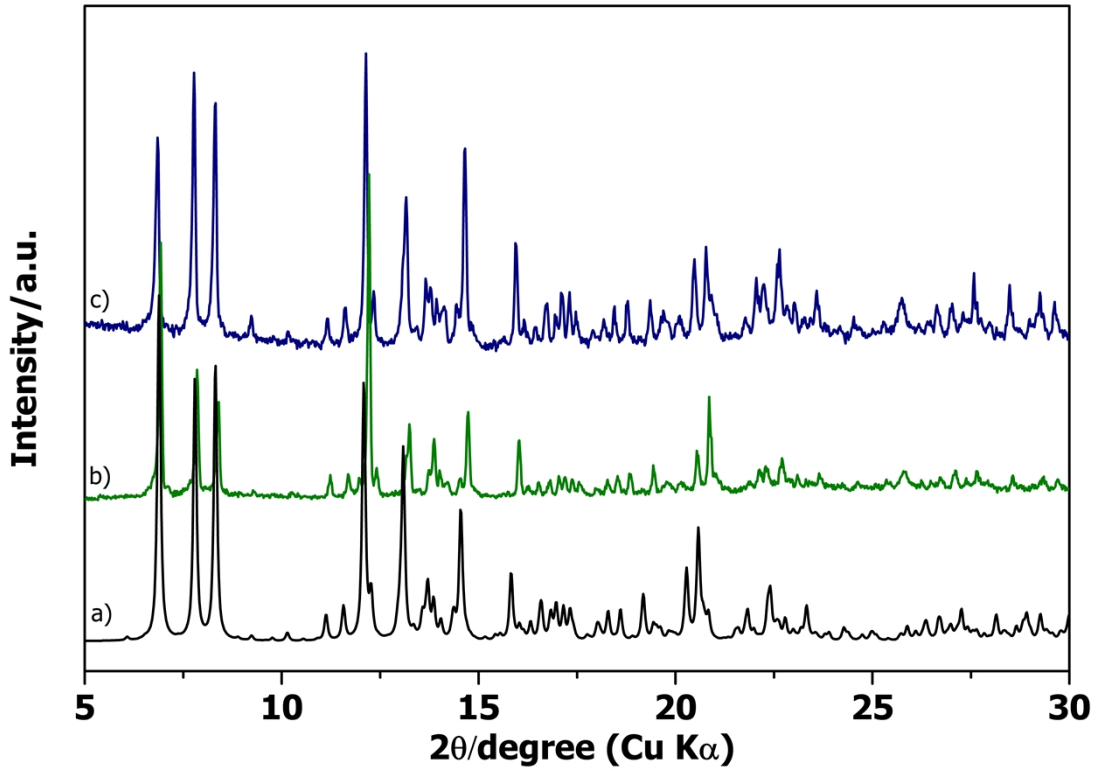


Fig. S17 Normalized XRD patterns of InPF-15: a) simulated PXRD, b) Experimental PXRD and c) PXRD after the first run of cyanosilylation catalysis.

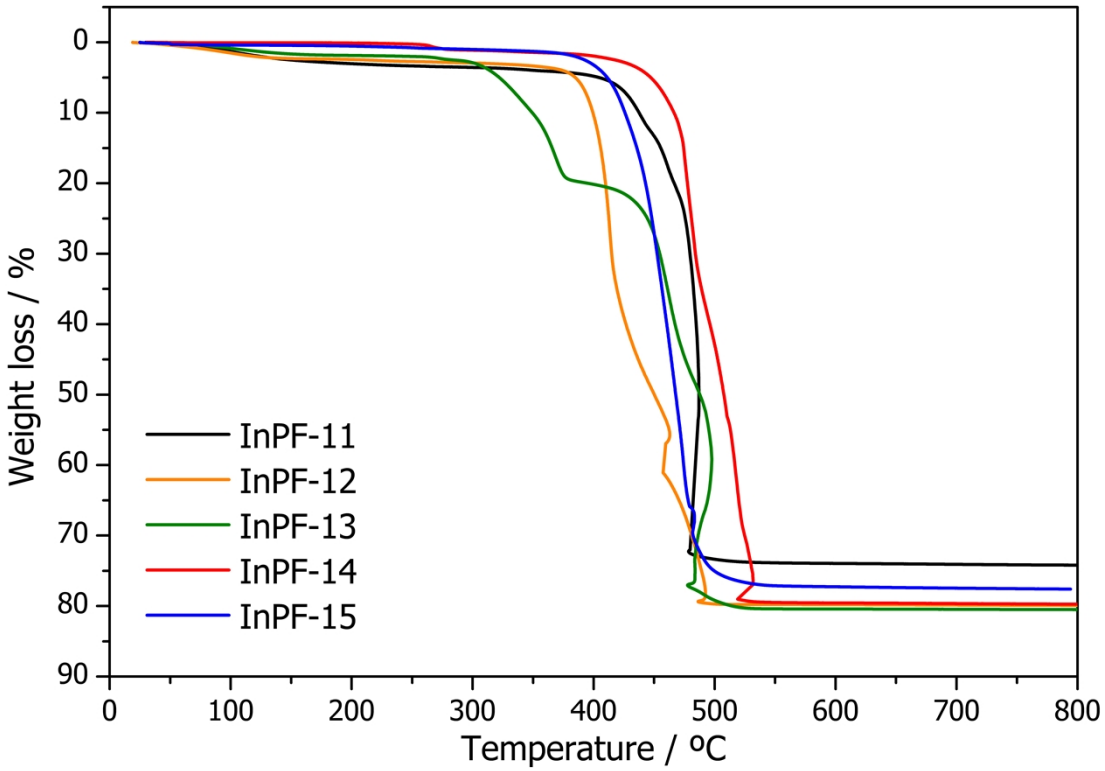


Fig. S18 TGA profiles of InPF-11 to InPF-15 compounds performed in air (flow of 100 mL.min-1) with a heating rate of 10 ºC/min.

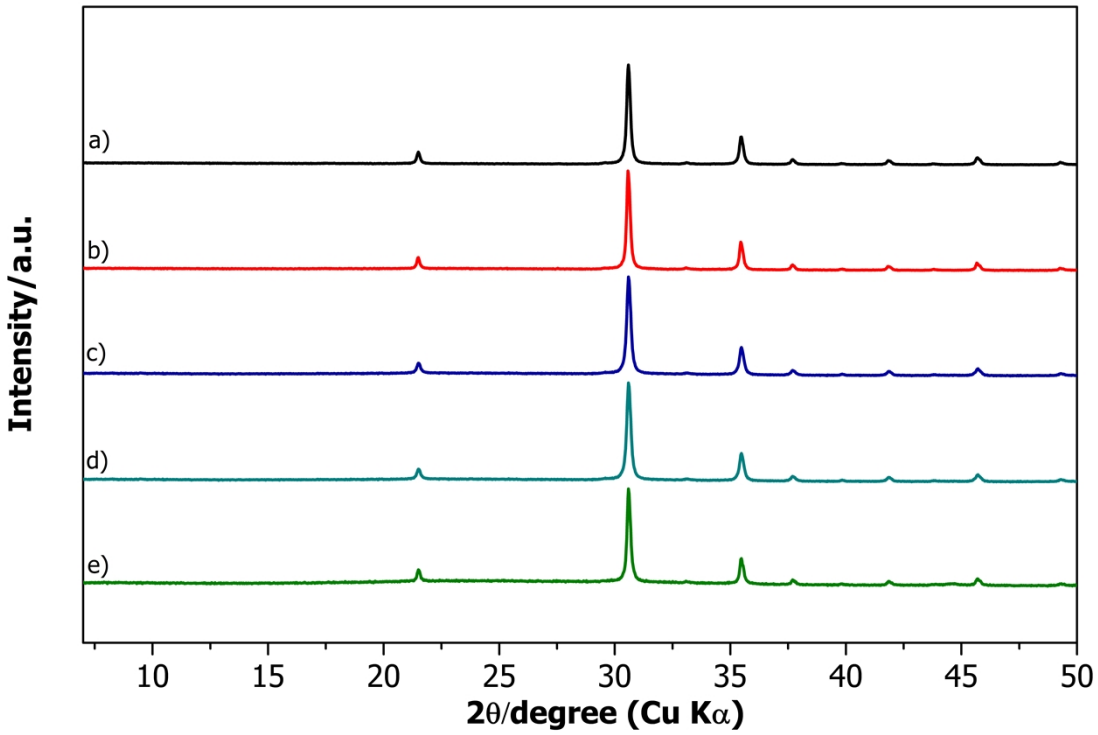


Fig. S19 PRXD profiles for TGA residues of indium catalysts: a) InPF-11, b) InPF-12, c) InPF-13, d) InPF-14 and e) InPF-15. The final residue at 800ºC for all catalysts is pure In2O3 (ICSD_640179), confirmed by XRPD.

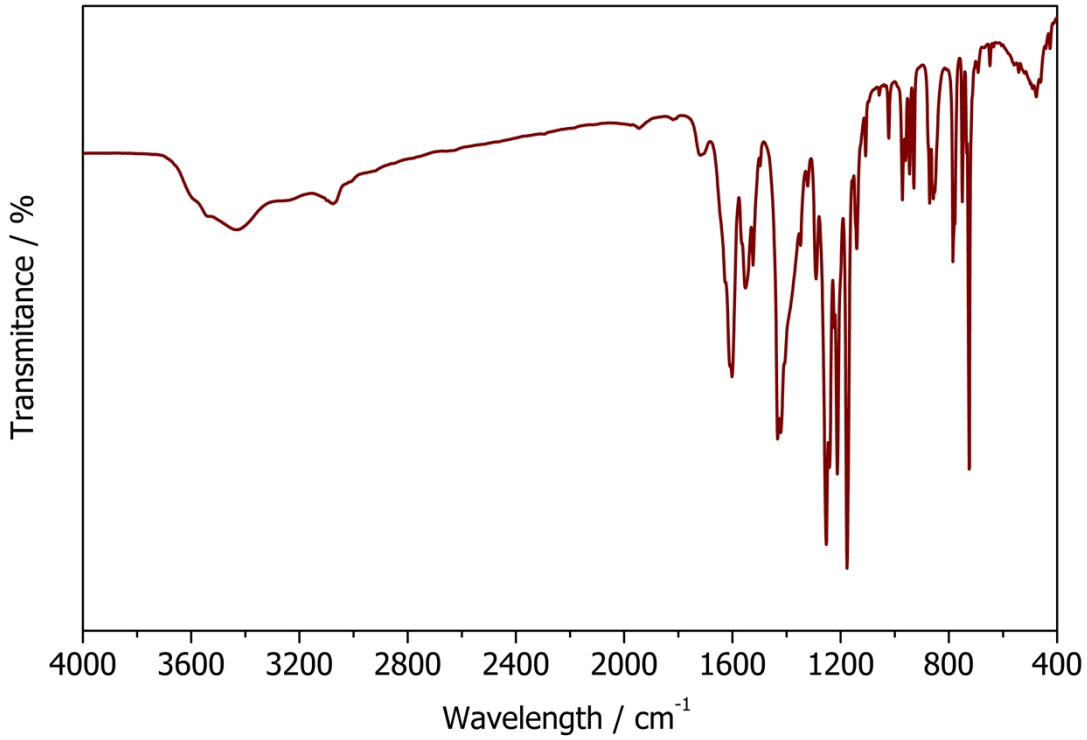


Fig. S20 FTIR spectra of compounds InPF-12 in the 4000-300 cm-1 range.

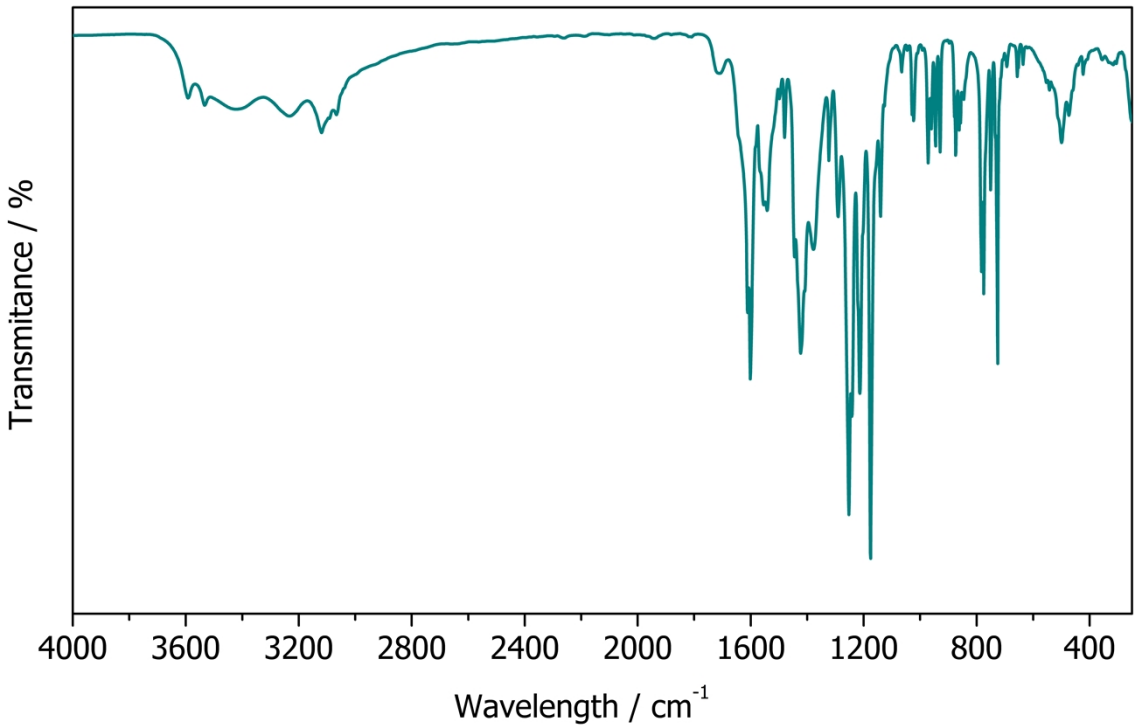


Fig. S21 FTIR spectra of compounds InPF-13 in the 4000-300 cm-1 range.

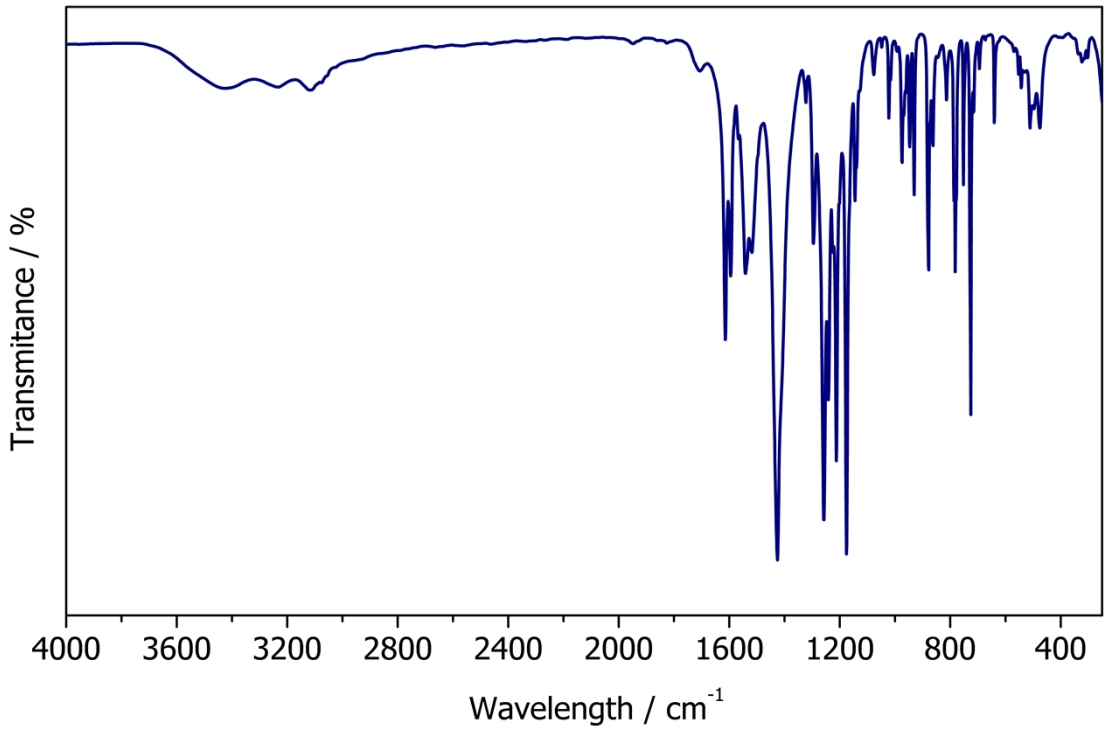


Fig. S22 FTIR spectra of compounds InPF-14 in the 4000-300 cm-1 range.

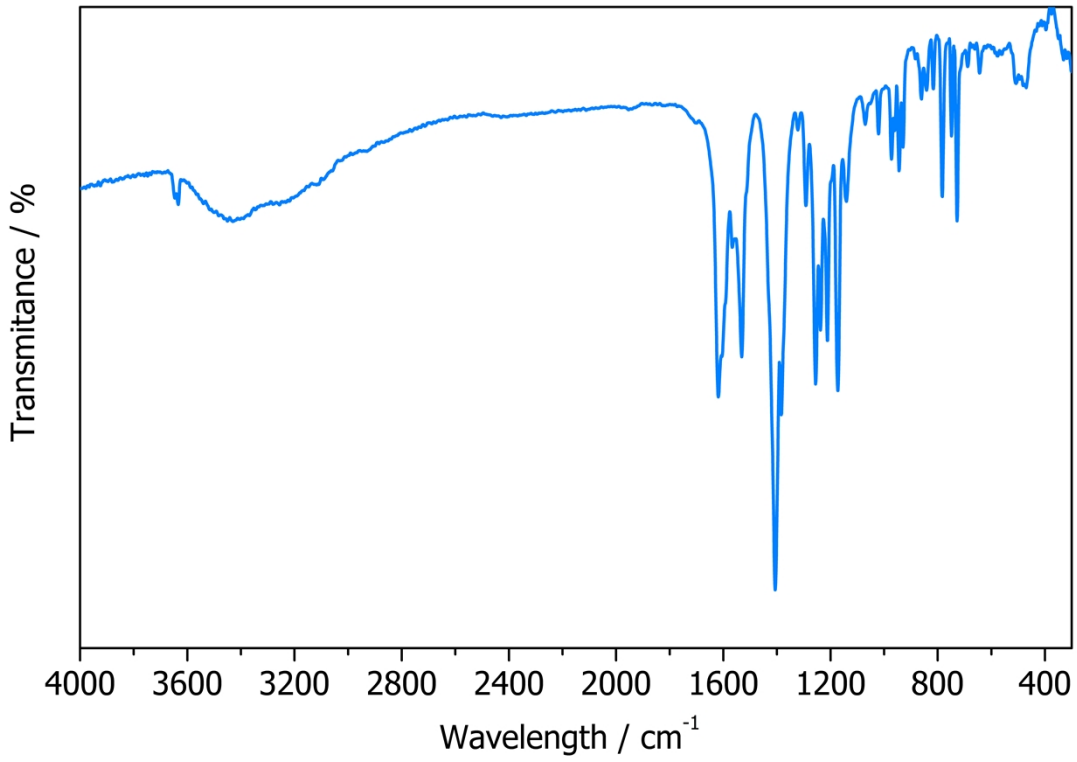


Fig. S23 FTIR spectra of compounds InPF-15 in the 4000-300 cm-1 range.

**References**

1 APEX2; Bruker-AXS: Madison, WI, 2006.
2 Siemens SAINT Data Collection and Procedure Software for the SMART System, Siemens Analytical X-ray Instruments, Inc., Madison, WI, 1995.
3 Siemens SHELXTL, Version 5.0, Siemens Analytical X-ray Instruments Inc., Madison, WI, 1995.
4 Software for the SMART System V5. 0.4 and SHELXTL V 5.1, Bruker-Siemens Analytical X-ray Instrument Inc., Madison, WI, 1998.
5 Inorganic Crystal Structure Database, ICSD.